9

Simulating Effects of Climate and Vegetation Change on Distributions of Martens and Fishers in the Sierra Nevada, California, Using Maxent and MC1

Wayne D. Spencer, Heather Rustigian-Romsos, Ken Ferschweiler, and Dominique Bachelet

ABSTRACT

We used Maxent distribution models and MC1 to investigate effects of climate and vegetation on the distribution of martens (*Martes caurina*) and fishers (*Pekania pennanti*) in the Sierra Nevada, California, under current and projected future conditions. Both species are forest carnivores of conservation concern in California, where they reach their southernmost distributions. The species occupy similar ecological niches and may compete in the elevation band where their ranges overlap—but martens mostly occupy higher elevations with deep, persistent snow, and fishers occupy lower elevations with less snow. We systematically varied types of environmental variables (climate, vegetation, terrain, presence or absence of the other species) included in Maxent models and compared area-under-curve (AUC) values to determine what variables best predict current distributions. Terrain variables and presence or absence of the competing species did not add significantly to model fit. For fishers, models using both climate and vegetation variables outperformed those using only vegetation; for martens, there was no significant difference between vegetation-only, climate-only, and vegetation + climate models. We then prepared climate + vegetation Maxent models using MC1-derived variables that best approximated the variables used in the best current (benchmark) models, compared predicted distributions with benchmark models, and projected distributions to mid- and late 21st century using MC1 vegetation projections and an array of downscaled general circulation models (GCMs) and emission scenarios at three resolutions (10 km, 4 km, 800 m). The finest available GCM resolution (800 m) provided the best spatial congruence between MC1-derived models and benchmark models. Regardless of GCM emission scenario, predicted marten distribution shifted to higher elevations, became more fragmented, and decreased in area by 40−85% (depending on scenario) compared to current distributions. Predicted changes in fisher distribution were more variable across GCM scenarios, with some increases and some decreases in extent and no consistent elevation shifts—suggesting high uncertainty in climate change effects on fishers. Management to benefit these species should consider ways of sustaining appropriate vegetation conditions within their preferred climate envelopes via adaptive management.

9.1. INTRODUCTION

Predicting how climate change may affect wildlife species requires understanding how their distributions are influenced by climate, vegetation, other species, and other habitat factors at various spatial and temporal resolutions, as well as how conditions may change in the future. We modeled the current and future distributions of two species of conservation concern in California that may compete with one another—martens (*Martes caurina*) and fishers (*Pekania pennanti*)—using Maxent distribution modeling software [*Phillips et al.*, 2006; *Elith et al.*,

Conservation Biology Institute, Corvallis, Oregon, USA

Global Vegetation Dynamics: Concepts and Applications in the MC1 Model, Geophysical Monograph 213, First Edition.
Edited by Dominique Bachelet and David Turner.

2011] and the dynamic vegetation model MC1 [*Bachelet et al*., 2001], which is described thoroughly in Chapter 1 of this book. We assessed how the current distributions of these species are affected by climate variables, vegetation variables, terrain variables, and the presence or absence of the other species. We used the results of these analyses to inform models projecting the species' future distributions using vegetation change projections from MC1 and multiple general circulation models (GCM), emission scenarios, and resolutions. The results can inform climate change vulnerability assessments and conservation plans for these species. They also illustrate how MC1 can be used in projecting future species distributions, and the importance of considering how the spatial resolution of downscaled climate futures may affect these projections.

Martens and fishers are forest carnivores that reach their southernmost distributions in the Sierra Nevada mountain range in California [*Zielinski et al*., 2005]. Their populations declined significantly over about the past 100–150 years, due largely to habitat alteration by logging, grazing, and other human influences. Both are considered species of conservation concern by state and federal agencies, and the fisher is a candidate for listing under the California and US Endangered Species Acts. The species have similar ecological niches within slightly overlapping elevation zones—with the smaller marten occupying subalpine forests that experience deep and persistent snow, and the larger fisher occupying midelevation forests that experience less snow and warmer temperatures [*Krohn et al*., 1997]. Because martens and fishers require similar forest structural conditions (dense, structurally complex forests with large trees and abundant dead wood) [*Purcell et al*., 2012] but different climate regimes (cooler, moister, and snowier conditions for martens; warmer, drier, and less snowy conditions for fishers) [*Krohn et al*., 1997, 2004], they offer a unique opportunity to investigate how climate change may affect them directly as well as through changes in vegetation. Also, because they compete with one another for food where their ranges overlap [*Zielinski and Duncan*, 2004], and fishers sometimes kill martens when they meet [*Krohn et al*., 2004], this system offers an opportunity to investigate how species interactions may affect future populations. The availability in California of downscaled GCM projections at several resolutions presented an opportunity to also assess how spatial resolution may affect projections of future species distributions—an important concern in climate vulnerability assessments [*Franklin et al*., 2012].

9.2. METHODS

We used Maxent software to produce and evaluate species distribution models—and MC1 and several downscaled GCM projections to project future vegetation and climate conditions—using a multistep process to analyze current and future species distributions. First, we systematically varied the types of environmental variables included in Maxent distribution models to determine what factors best predict these species' distributions under current conditions. Specifically, we investigated how current distributions of martens and fishers are influenced by vegetation characteristics (e.g., forest composition and structure), climate (e.g., temperature, precipitation, snow depth and duration), terrain variables (e.g., elevation, slope), and the presence or absence of the other species. The goal of these analyses was to determine what types of variables best explain their current distributions (i.e., whether they are selecting primarily on the basis of local climatic conditions, vegetation characteristics, terrain, the presence or absence of the other species, or combinations of these or other factors).

The results of the current distribution analyses were then used to inform variable selection for models projecting possible future distributions to make predictions about the vulnerability of these species to changes in climate and vegetation. Specifically, we used MC1 to simulate recent (1986–2005) and future (2046–2065 and 2076–2095) vegetation conditions on the basis of climate projections from several emission scenarios downscaled at three spatial resolutions (800 m, 4 km, and 10 km). We created Maxent distribution models for these time periods by selecting environmental variables generated by MC1 that were similar to the variables that best predicted current species' distributions. We compared the recent MC1-based models with our current best (or benchmark) models to determine how well the MC1-based models predicted species' distributions at each resolution, and then compared how predicted distributions may shift in the future with climate and vegetation changes.

For each Maxent model, we inspected the permutation importance and univariate and marginal response curves for each variable to understand the relative contributions of each variable, or combinations of variables, to model performance, and what ranges of variable values the species were selecting for or against [*Phillips*, 2006]. We used $p < 0.05$ as significance threshold for all statistical tests.

9.2.1. Current Species Distributions

For each species, we created and compared a wide array of potential distribution models using Maxent with default settings, relevant environmental predictors (available at 800 × 800-m resolution for climate variables and 100 × 100 m for other variables) (Table 9.1), and marten and fisher localities from two sources: the California Natural Diversity Data Base [*CNDDB*, 2011] and data compiled by the USDA Forest Service from a variety of survey and monitoring studies (R. Schlexer, USDA

Table 9.1 Predictors used in current conditions models.

Current vegetation (*sources*: existing vegetation, USDA Forest Service, Pacific Southwest Region, Remote Sensing Lab, 2005–2009; vector, minimum mapping unit of 2.5 acres; FVEG, California Department of Forestry and Fire Protection, Fire and Resource Assessment Program, 2006, raster, 30 m)	
CWHR2[a,h]	Fisher CWHR[a] rating (arithmetic mean of REPRODUCTION, FEEDING, COVER) 100, excluding CWHR types red fir, lodgepole pine, subalpine conifer, and montane riparian
DFOR2[a]	Proportion of moving window with CWHR-type montane hardwood-conifer, montane hardwood, ponderosa pine, Douglas fir, Sierran mixed conifer, Jeffrey pine, white fir, aspen, or eastside pine *and* CWHR density *D* (60–100% canopy closure)
DLFOR[a]	Proportion of moving window with CWHR-type montane hardwood-conifer, montane hardwood, ponderosa pine, Douglas fir, Sierran mixed conifer, Jeffrey pine, white fir, aspen, or eastside pine and CWHR density *D* (60–100% canopy closure) and CWHR size 4, 5, or 6 (>28 cm dbh)
HREPRO[a,h]	Proportion of moving window with fisher CWHR reproduction rating high
KHREPRO[bi]	Proportion of moving window with marten CWHR reproduction rating high (modified by *Kirk and Zielinski* [2009]), CWHR-type lodgepole pine, red fir, subalpine conifer, white fir, or montane riparian, *and* CWHR size 4, 5, or 6 (>28 cm dbh), *and* CWHR density *M* or *D* (≥40% canopy closure)
LPN	Proportion of moving window with CWHR-type lodgepole pine *and* CWHR size 4, 5, or 6 (>28 cm dbh), *and* CWHR density *M* or *D* (≥40% canopy closure)
LRGFOR[a]	Proportion of moving window with CWHR- type montane hardwood-conifer, montane hardwood, ponderosa pine, Douglas fir, Sierran mixed conifer, Jeffrey pine, white fir, aspen, eastside pine, *and* CWHR size 4, 5, or 6 (>28 cm dbh)
LRGHDWD[c]	Proportion of moving window with CWHR-type montane hardwood *or* montane hardwood-conifer *and* CWHR size 3, 4, 5, or 6 (>15 cm dbh)
MSTRUCT[d]	Score averaged over the moving window, which is the product of the following three factors: habitat indicator variable (1 for Sierran mixed conifer, white fir, red fir, or lodgepole pine; 0 otherwise); forest canopy closure [centroid of class interval: *S* (10–24%) = 17.5, *P* (25–39%) = 32, *M* (40–59%) = 50, and *D* (≥60%) = 80)]; tree size [centroid of class interval: 1 (0–2.5 cm dbh) = 0.5, 2 (2.5–15 cm dbh) = 3.5, 3 (15–28 cm dbh) = 8.5, 4 (28 – 61 cm dbh) = 17.5, 5 (>61 cm dbh) = 24, and 6 (multilayered trees) = 37]
MSTRUCT2[b]	Score averaged over the moving window, which is the product of the following three factors: habitat indicator variable (1 for red fir, or lodgepole pine; 0 otherwise); forest canopy closure [centroid of class interval: *S* (10–24%) = 17.5, *P* (25–39%) = 32, *M* (40-59%) = 50, and *D* (≥60%) = 80)]; tree size [centroid of class interval: 1 (0–2.5 cm dbh) = 0.5, 2 (2.5–15 cm dbh) = 3.5, 3 (15–28 cm dbh) = 8.5, 4 (28–61 cm dbh) = 17.5, 5 (>61 cm dbh) = 24, and 6 (multilayered trees) = 37]
PHDWD[c]	Proportion of moving window with CWHR-type montane hardwood or montane hardwood-conifer, or secondary type riparian mixed hardwood, interior mixed hardwood, canyon live oak, black oak, interior live oak, black cottonwood, or montane mixed hardwood
RFR[b]	Proportion of moving window with CWHR-type red fir *and* WHR size 4, 5, or 6 (>28 cm dbh), *and* CWHR density *M* or *D* (≥40% canopy closure)
SMC[d]	Proportion of moving window with CWHR-type Sierran mixed conifer *and* WHR size 4, 5, or 6 (>28 cm dbh), *and* CWHR density *M* or *D* (≥40% canopy closure)
STRUCT[a]	Score (from *Davis et al.* [2007]) averaged over the moving window, which is the product of the following three factors: habitat indicator variable (1 for montane hardwood-conifer, montane hardwood, ponderosa pine, Douglas fir, Sierran mixed conifer, Jeffrey pine, white fir, aspen, eastside pine, red fir, lodgepole pine, subalpine conifer, or montane riparian; 0 otherwise); forest canopy closure [centroid of class interval: *S* (10–24%) = 17.5, *P* (25–39%) = 32, *M* (40–59%) = 50, and *D* (≥60%) = 80]; tree size [centroid of class interval: 1 (0–2.5 cm dbh) = 0.5, 2 (2.5–15 cm dbh) = 3.5, 3 (15–28 cm dbh) = 8.5, 4 (28–61 cm dbh) = 17.5, 5 (>61 cm dbh) = 24, and 6 (multilayered trees) = 37]
STRUCT2[a]	Score averaged over the moving window, which is the product of the following three factors: habitat indicator variable (1 for montane hardwood-conifer, montane hardwood, ponderosa pine, Douglas fir, Sierran mixed conifer, Jeffrey pine, white fir, aspen, or eastside pine; 0 otherwise); forest canopy closure [centroid of class interval: *S* (10–24%) = 17.5, *P* (25–39%) = 32, *M* (40–59%) = 50, and *D* (≥60%) = 80)]; tree size [centroid of class interval: 1 (0–2.5 cm) = 0.5, 2 (2.5–15 cm) = 3.5, 3 (15–28 cm) = 8.5, 4 (28–61 cm) = 17.5, 5 (>61 cm) = 24, and 6 (multilayered trees) = 37]
WFR	Proportion of moving window with CWHR-type white fir *and* CWHR size 4, 5, or 6 (>28 cm dbh), *and* CWHR density *M* or *D* (≥40% canopy closure)
Terrain (*source*: National Elevation Dataset, US Geological Society, 2009, raster, 1 arc-second)	

(*Continued*)

Table 9.1 (*Continued*)

ADJELEV[e]	Latitude-adjusted elevation (from *Davis et al.* [2007]) averaged over the moving window: 0.625 m was added to elevation for every 1 km north from the southernmost point in the study area
INSOL_IND[f]	Solar insolation index (from *Gustafson et al.* [2003]) derived from slope and aspect and averaged over the moving windows = 2 – (sin((slope/90)180))*(cos(22 – aspect) + 1)
PSLOPE[f]	Mean percent slope over the moving window
RELIEF[f]	Mean value of local relief over the moving window, calculated as the standard deviation of elevation in a local 5 × 5 moving window
SW	Mean value over the moving window of transformed slope aspect (from *Franklin* [2003]): cos(aspect-255)
VRM[f]	Mean over the moving window of the vector ruggedness measure (from *Sappington et al.* [2007]), which quantifies terrain ruggedness using vector analysis to capture variability in slope and aspect into a single variable; values can range from 0 to 1 but typically don't exceed 0.4
Current climate (1986–2005; *source*: PRISM Climate Group, Oregon State University, http://prism.oregonstate.edu, raster, 857.5 m)	
PPT[g]	Mean annual precipitation (mm) over the moving window
SNOWI[e]	Number of months per year with average temperature < 0°C averaged over the moving window
SNOWI2[e]	Mean amount of precipitation (mm) per year that fell in months with mean temperatures < 0°C averaged over the moving window
SUMMPPT	Mean annual summer (July– Sept.) precipitation (mm) averaged over the moving window
SUMMTAMP	Mean difference between maximum temperature and minimum temperature (°C) during summer months (July–Sept.) averaged over the moving window
SUMMTMAX[e]	Mean summer (July–Sept.) maximum temperature (°C) averaged over the moving window
TMAX[e]	Mean of the maximum temperature (°C) value for the month with the highest maximum temperature value each year (the month that got hottest) averaged over the moving window
TMIN[e]	Mean of the minimum temperature (°C) value for the month with the highest minimum temperature value each year (the month that didn't get cold) averaged over the moving window
WINTPPT[g]	Mean annual winter (Jan.–March) precipitation (mm) averaged over the moving window
WINTTMIN[e]	Mean winter (Jan.–March) minimum temperature (°C) averaged over the moving window

[a–g] Highly correlated variables ($|r| > 0.85$)
[h] Variables used only in fisher models
[i] Variables used only in marten models.

Forest Service, Pacific Southwest Research Station, unpublished data). All environmental predictor layers were smoothed with a 10-km^2 moving window because we have found in previous analyses [*Spencer et al.*, 2015; *Zielinski et al.*, 2015] that this moderate resolution performs well across most variables and both species, and it is biologically justified as approximating the habitat area needed to support one to a few individuals of each species. Prior to modeling, species locality data were filtered to remove redundant observations (i.e., the same observation repeated in multiple data sources), historical observations (pre-1990), and observations not considered highly reliable (i.e., not supported by physical evidence, such as museum specimens, captures, photographs, or tracks). The detection datasets were further filtered for spatial independence (i.e., to avoid including multiple observations of the same individual and minimize bias due to spatial clumping of sampling effort) using a nearest-neighbor algorithm approximating home range diameter of the species. If two marten observations were <3 km apart or two fisher localities were <5 km apart, the older or less reliable observation was removed.

We calculated correlations between each pair of environmental variables to avoid including highly correlated variables ($|r| > 0.85$) within a model (e.g., we might use total annual precipitation or total winter precipitation in a model, but not both). We then ran univariate Maxent models for each species with each variable. Using variables that yielded the highest 10-fold cross-validated AUC values (area under the receiver operating curve; a measure of model fit that varies from 0 to 1.0 [*Fielding and Bell*, 1997] and omitting any variables with AUC < 0.7, we then created alternative Maxent models by combining variables into six different model classes: (1) climate only, (2) vegetation only, (3) climate + vegetation, (4) climate + vegetation + terrain, (5) climate + vegetation + presence/absence of the other species, and (6) climate + vegetation + terrain + presence/absence of the other species.

We compared the resulting multivariate models statistically to determine which factors most strongly predict species' distributions. Specifically, we compared 10-fold cross-validated AUCs using one-way ANOVA, Tukey HSD tests, and *t* tests to determine the best predictive models. The relative contributions of variables to model performance were evaluated using *permutation performance*, a measure of predictive power provided by Maxent software and defined as the decrease in training AUC, normalized to percentages, resulting from random permutation in variable values at training presence and background points [*Elith et al.*, 2011]. The final best current distribution models for each species were used as benchmarks against which to evaluate the performance of models built with predictors produced by the MC1 vegetation model.

9.2.2. Future Projections

The analysis of current distribution models suggested that climate + vegetation models, at scales corresponding roughly with species' home range sizes, were strong predictors of species distributions, but that terrain variables and presence or absence of the competing species did not add significantly to model fit. Informed by these analyses, we next created climate + vegetation models using the same process as above and variables from the MC1 global vegetation model (Table 9.2), which can be projected into the future. The future distribution models used projections from five different climate models/emissions scenarios at three spatial resolutions (800 m, 4 km, and 10 km) averaged over three, 20-year time periods (contemporary, 1986–2005; midcentury, 2046–2065; and late century, 2076–2095):

- PCM1 [*Washington et al.*, 2000; *Meehl et al.*, 2003] A2 (*Nakićenović et al.*, 2000) (10 × 10 km; from *Lenihan et al.* [2008])
- Hadley CM3 [*Gordon et al.*, 2000; *Pope et al.*, 2000] A1Fi (10 × 10 km; from *Hayhoe et al.* [2004])
- MIROC 3.2 medres [*Hasumi and Emori*, 2004] A2 [*Nakićenović et al.*, 2000] (4 × 4 km and 800 × 800 m)
- Hadley CM3 [*Johns et al.*, 2003] A2 [*Nakićenović et al.*, 2000] (4 × 4 km and 800 × 800 m)
- CSIRO Mk3 [*Gordon*, 2002] A2 [*Nakićenović et al.*, 2000] (800 × 800 m)

Results of the MC1-based distribution models for the contemporary time period at the three different resolutions were compared with the benchmark models to determine whether they gave comparable results and were therefore

Table 9.2 Predictors used in MC1-based distribution models. Superscript letters indicate highly correlated variables ($|r| \geq 0.85$).

Vegetation (simulated with MC1)	
BURN	Mean fraction of vegetation carbon burned
COARSEWOOD	Mean fraction of total forest carbon in coarse wood carbon (4 × 4 km only)
FORC	Mean total forest ecosystem carbon (g C/m^2)
FORFRACT	Mean ratio of total (aboveground and belowground) tree biomass over total ecosystem biomass; index of "woodiness"
FORIND	Mean ratio of total (aboveground and belowground) grass biomass over total tree biomass; index of understory density and fine fuels (800 × 800 m and 10 × 10 km only)
MAXTREE	Average maximum tree LAI (m^2/m^2)
VCLASS	Dominant (modal) vegetation class
VEGC	Mean vegetation carbon (g C m^2)
VTYPE	Dominant (modal) vegetation type (800 × 800 m and 4 × 4 km only)
Climate (simulated with MC1)	
MARCHSNOW	Mean amount of snow (mm) on the ground in March (800 × 800 m and 4 × 4 km only)
PET	Mean potential evapotranspiration (mm) (800 × 800 m and 4 × 4 km only)
Climate (*sources*: Climate Group, Oregon State University (http://prism.oregonstate.edu) and *Meehl et al.* [2007])	
PPT	Mean annual precipitation (mm)
SNOWI	Mean number of months per year with average temperature < 0°C
SNOWI2	Mean amount of precipitation (mm) per year that fell in months with mean temperatures < 0°C
SUMMPPT	Mean summer (July–Sept.) precipitation (mm)
SUMMTAMP	Mean difference between maximum and minimum temperatures (°C) during summer (July–Sept.)
SUMMTMAX	Mean summer (July–Sept.) maximum temperature (°C)
TMAX	Mean maximum temperature (°C)
TMIN	Mean minimum temperature (°C)
WINTPPT	Mean winter (Jan.–March) precipitation (mm)
WINTTMIN	Mean winter (Jan.–March) minimum temperature (°C)

reliable predictors of marten and fisher distributions. Specifically, we compared predicted distribution—defined as predicted probability of occurrence greater than or equal to the maximum sensitivity plus specificity threshold provided by Maxent [*Liu et al.*, 2013]—using the spatial congruence index [*Legendre and Legendre*, 1998; *Franklin et al.*, 2012]. The best-resolution MC1-based models were then projected to the mid- and late-century time periods under each emission/global circulation scenario. We calculated net change in predicted distribution relative to the contemporary time period and stable range (percent of contemporary distribution remaining suitable) at each time period to assess the potential vulnerability of marten and fisher to projected climate change.

9.3. RESULTS

9.3.1. Current Species Distributions

The distributions of martens and fishers were well predicted by both vegetation-only and climate-only models (all AUCs > 0.8), but models combining both vegetation and climate variables performed significantly better than did models based on vegetation alone for fishers. There was no significant difference between the vegetation + climate model and the climate-only or vegetation-only marten models (Table 9.3). Terrain variables were not included in multivariate models for either species due to poor univariate performance (all AUCs < 0.7). For both species, the presence/absence of the other species did not improve model predictive power relative to vegetation + climate models.

Table 9.3 AUC values for different model types for predicting current distributions of martens and fishers.

Model	Fisher	Marten
VEG	0.809	0.836
CLIM	0.824	0.837
VEG + CLIM	0.871[a]	0.858
VEG, CLIM, + TERR	NA[b]	NA[b]
VEG, CLIM, + SPECIES	0.865	0.858
VEG, CLIM, TERR, + SPECIES	NA[b]	NA[b]

[a] Significantly better than vegetation-only model ($P < 0.05$).
[b] No terrain or species variables met the univariate AUC ≥ 0.7 cutoff to be entered into multivariate model.

The best marten model included two climate predictors and four vegetation variables (Table 9.4). Climate variables (annual precipitation and mean maximum temperature) accounted for 74.1% of permutation importance, with mean maximum temperature contributing the most (56.1%). These results and inspection of response curves indicate that martens are strongly associated with areas experiencing low maximum temperatures and high annual precipitation that also support structurally complex forests and abundant lodgepole pine.

The best fisher model included three vegetation and three climate predictors (Table 9.4), with vegetation predictors accounting for 57.6% of permutation importance. STRUCT (an index of forest structure based on tree size and canopy cover classes) was the dominant vegetation contributor, with a permutation importance of 38.2% (followed by proportions of area classified as Sierran mixed-conifer and hardwood vegetation types). Together the three climate variables (summer temperature amplitude, mean winter precipitation, and mean summer precipitation) contributed 44.4% of permutation importance. These results and inspection of response curves indicate that fishers are associated with dense forests supporting large mixed conifers and some hardwoods, in areas with moderate summer temperatures and low to moderate precipitation in both winter and summer.

Table 9.4 Variables included in best models for current conditions, including the benchmark models and the MC1-based models at three resolutions.

Species	Current Conditions[a] (Benchmark)	800 m	4 km	10 km
Marten	LPN, MSTRUCT, MSTRUCT2, STRUCT	BURN, FORC, FORFRACT, FORIND, MAXTREE, VCLASS	BURN, COARSEWD, FORC, FORFRACT, FORIND, MAXTREE, VCLASS	BURN, FORIND, VCLASS, VEGC
	PPT, TMAX	PET, PPT	MARCHSNOW, WINTPPT	PPT, SUMMPPT, SUMMTAMP, TMAX
Fisher	PHDWD, SMC, STRUCT	FORC, FORFRACT, FORIND	COARSEWD, FORC, FORFRACT, FORIND, VCLASS	BURN, VCLASS, VEGC
	SUMMPPT, SUMMTAMP, WINTPPT	PPT, SUMMTAMP	SNOWIND, SUMMPPT, SUMMTAMP, WINTPPT	SUMMPPT, SUMMTAMP, TMIN, WINTPPT

[a] Variables averaged over a 10-km^2 moving window.

9.3.2. Current Distributions Using MC1-Based Variables

Of three resolutions available for MC1 results, the finest (800 × 800-m) resolution performed best at predicting the contemporary distributions of both martens and fishers (Figure 9.1 and Table 9.5). The 10 × 10-km model appears to grossly overestimate marten distribution compared with the benchmark model (by an average of 1.4 times as much area), while underpredicting fisher distribution (average range ratio of 0.62, Figure 9.2). Model performance was very good at 800-m resolution (AUC values of 0.84 for both marten and fisher). However, MC1 variables performed better for martens than for fishers: the spatial congruence index between MC1-based distributions and benchmark models was 79% for martens and 60% for fishers, suggesting that MC1-based models are reasonably reliable predictors of marten distribution but less so of fisher distributions.

The best 800-m MC1-based marten model was dominated by two climate variables, annual precipitation and potential evapotranspiration (Table 9.4), which together accounted for 76.4% of the permutation importance. Vegetation variables contributed only 23.6% of permutation importance. These results and inspection of response curves show that the MC1-based models provide results similar to those for the marten benchmark model; they indicate that marten distribution is strongly associated with areas having low potential evapotranspiration and abundant annual precipitation that also support high forest biomass. They further suggest that martens are associated with forests that experience relatively low biomass losses to fires.

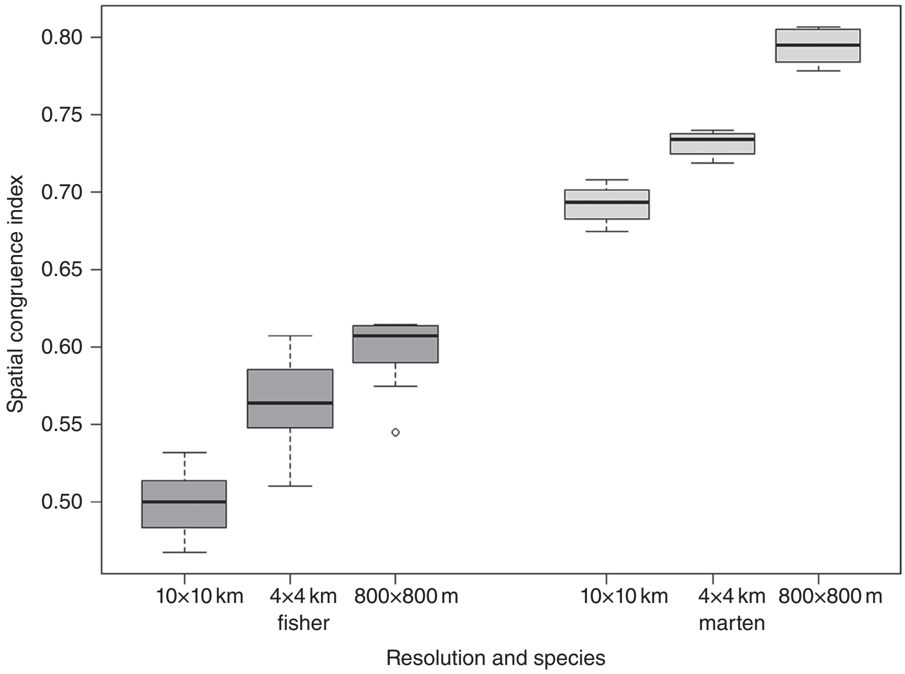

Figure 9.1 Influence of climate data resolution on spatial congruence of predicted contemporary species distributions for MC1-based Maxent models compared with the benchmark distribution models for martens and fishers.

Table 9.5 Mean spatial congruence index (SCI) values for best models at each resolution.

Species	Resolution	Mean SCI	t^a	df[a]	*p* Value[a]
Marten	800 × 800 m	0.79	—		—
	4 × 4 km	0.73	14.6219	16.125	2.002*e*–10
	10 × 10 km	0.69	20.9289	17.957	9.232*e*–14
Fisher	800 × 800 m	0.60	—		—
	4 × 4 km	0.57	2.8084	17.195	0.02398
	10 × 10 km	0.50	10.0411	17.866	1.804*e*–08

[a] Both *t* and *p* values (adjusted for two comparisons with the Bonferroni method) are compared to 800 m.

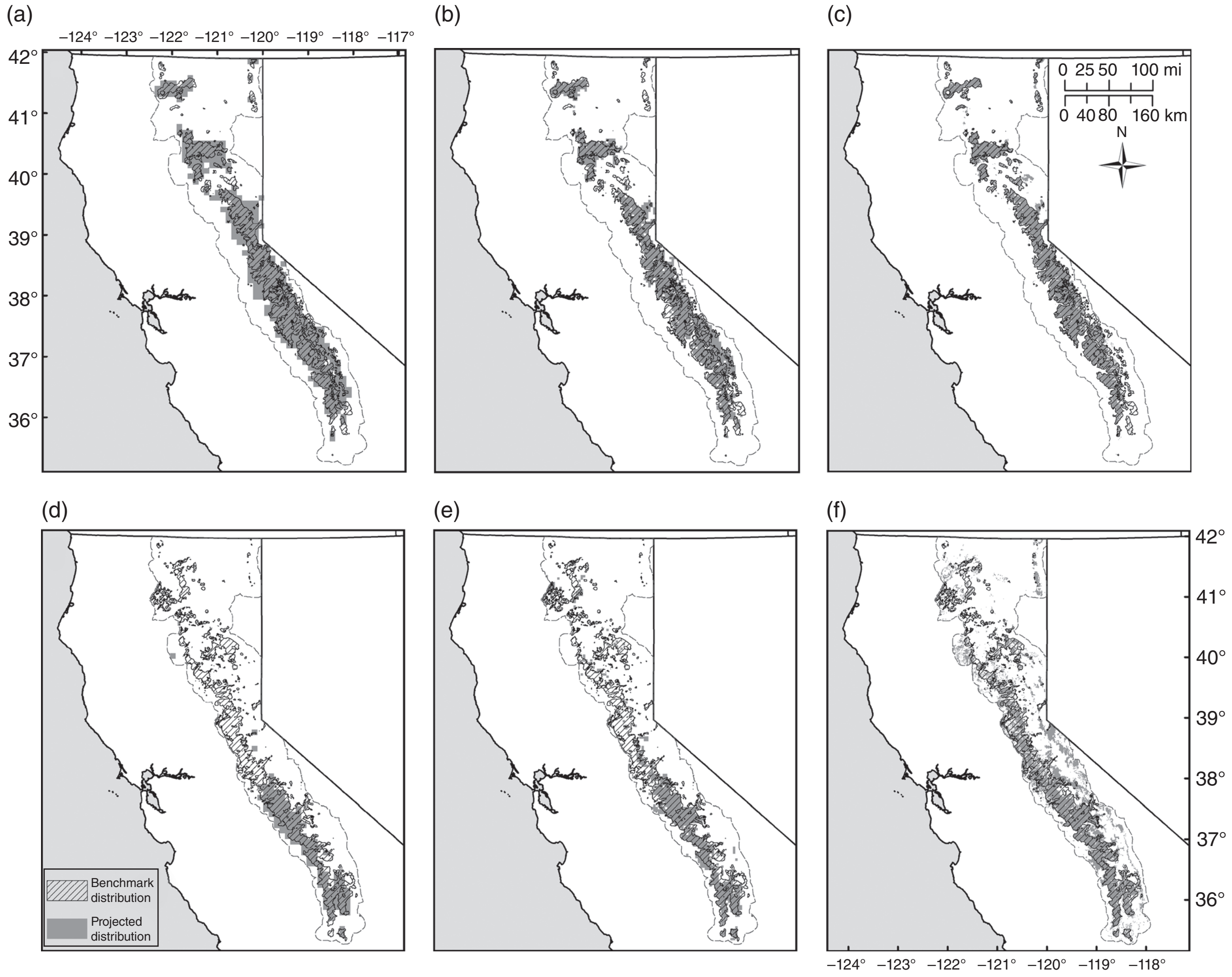

Figure 9.2 Maps of contemporary distributions for marten [top row, maps (a)–(c)] and fisher [bottom row, maps (d)–(f)] with resolution varying from coarsest [10 × 10 km, maps (a) and (d)] on the left, medium in the center [4 × 4 km, maps (b) and (e)], to finest on the right [800 × 800 m, maps (c) and (f)]. Hatched overlay shows the benchmark distribution based on the best current distribution models with 10-km^2 moving-window averaging.

The best 800-m MC1-based fisher model also provides results similar to those of the fisher benchmark model, with similar permutation importance of vegetation vs. climate variables and using different but related variables to represent suitable conditions. It was dominated by three vegetation variables (Table 9.4), which together accounted for 66.1% of permutation importance. Two climate variables, annual precipitation and summer temperature amplitude, contributed the remaining 33.9% of permutation importance. Similar to the benchmark model, these results and inspection of response curves support that fishers are associated with forests having high forest biomass in regions of the Sierra Nevada experiencing moderate amounts of precipitation and low amplitude in summer temperatures.

9.3.3. Future Projections

With all three GCM projections using the A2 emissions scenario (CSIRO Mk3, Hadley CM3, and MIROC 3.2 medres), Maxent models predict major contractions in marten distribution during the 21st century (net losses from 40% for CSIRO Mk3 to 85% for Hadley CM3) coupled with greatly increased fragmentation and generally upslope shifts in distribution (Figures 9.3−9.5). Only 11% (Hadley CM3) to 38% (CSIRO Mk3) of marten distribution is predicted to remain stable through the late 21st century. With the Hadley CM3 projections (Figure 9.4), models predict a major contraction in marten distribution by mid-21st century, followed by a slight expansion again by the end of the century, suggesting that there may

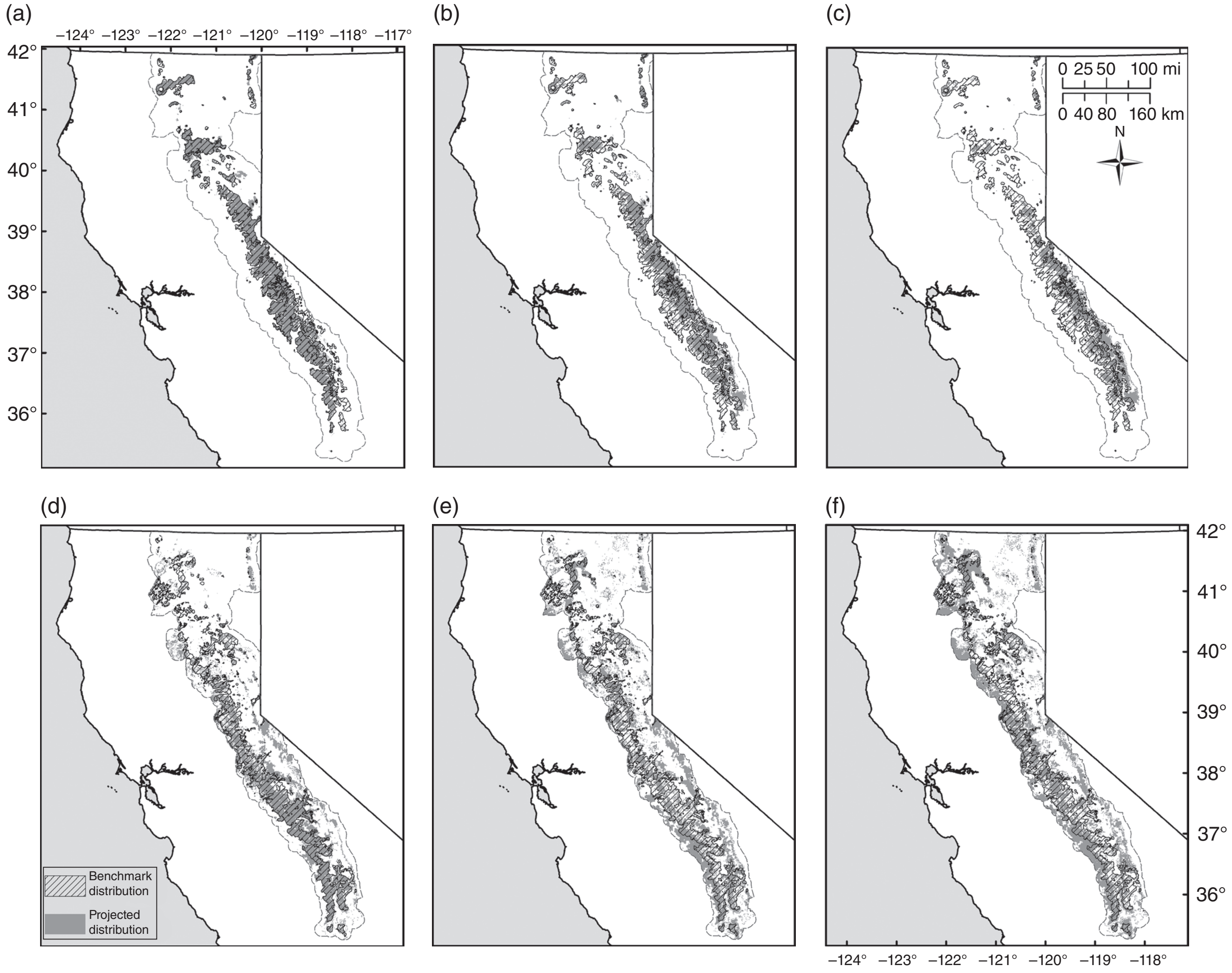

Figure 9.3 Predicted marten [top row, maps (a)–(c)] and fisher [bottom row, maps (d)–(f)] distributions under climate change projections from the CSIROMk3 GCM with the A2 emission scenario at 800 × 800-m resolution. Maps (a) and (d) show contemporary distributions (1986–2005); maps (b) and (e) show midcentury (2046–2065); maps (c) and (f) show late century (2076–2095). Hatched overlay shows the benchmark distribution based on the best current distribution models with 10-km^2 moving-window averaging. For color details, please see color plate section.

be a midcentury bottleneck that marten populations must pass through.

Predicted changes in fisher distribution were far more variable between GCMs than those for marten. By late 21st century, net changes in predicted fisher distribution range from a 33% loss (MIROC 3.2 medres) to a 38% gain (CSIRO Mk3), with 40% (MIROC 3.2 medres) to 60% of fisher distribution remaining stable through the late century (Table 9.6). There was also no consistent pattern of geographic or elevation shifts in the fisher projections. CSIRO Mk3 models project both downslope (generally westward) and upslope (eastward) expansion of fisher distribution along the length of the Sierra Nevada range (Figure 9.3), whereas the Hadley CM3 and MIROC 3.2 medres models project predominantly upslope shifts in the southern Sierra Nevada and both upslope and downslope expansion in the northern Sierra Nevada by late 21st century (Figures 9.4 and 9.5).

9.4. DISCUSSION

9.4.1. Current Species Distributions

Our results are consistent with previous findings that martens and fishers select structurally complex forest vegetation with dense canopies, large trees, and abundant

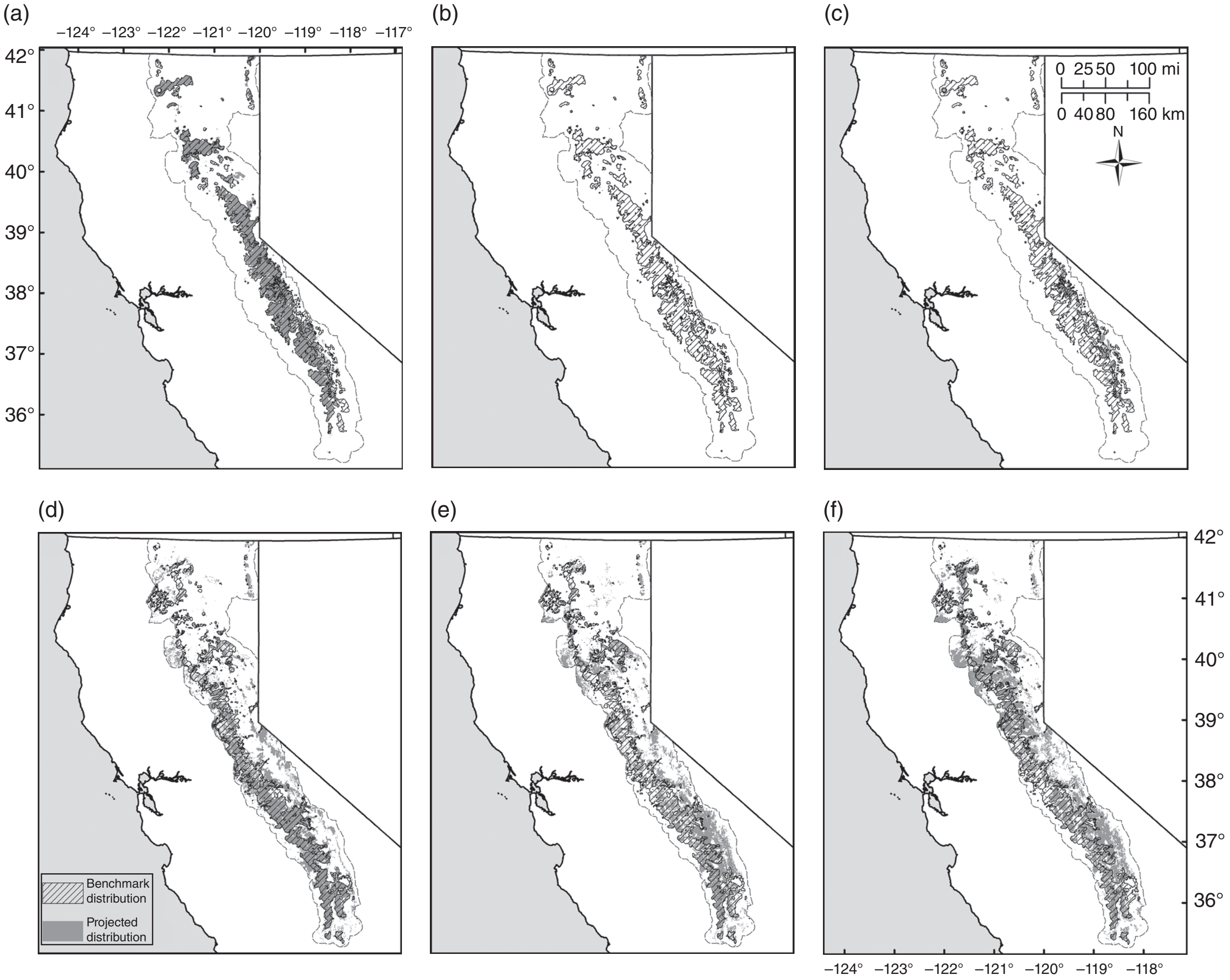

Figure 9.4 Predicted marten [top row, maps (a)–(c)] and fisher [bottom row, maps (d)–(f)] distributions under climate change projections from the HadCM3 GCM with the A2 emission scenario at 800 × 800-m resolution. Maps (a) and (d) show contemporary distributions (1986–2005); maps (b) and (e) show midcentury (2046–2065); maps (c) and (f) show late century (2076–2095). Hatched overlay shows the benchmark distribution based on the best current distribution models with 10-km^2 moving-window averaging. For color details, please see color plate section.

deadwood components, and that martens are associated with higher-elevation forest types (red fir, lodgepole pine) whereas fishers are associated with mid-elevation forest types (Sierran mixed conifers, mixed conifer-hardwoods) [*Purcell et al.*, 2012]. They also support that martens are better adapted to deep, soft, and persistent snow cover than fishers, due in part to lower foot-loading (ratio of body mass to total foot surface area)—which enables them to travel more easily on top of snow [*Krohn et al.*, 1997, 2004]—and a propensity to forage and rest under the snow when it is available [*Zielinski et al.*, 1983; *Spencer*, 1987].

Climate is a strong predictor of habitat characteristics for both species, but cannot account for vegetation disturbance history or other factors that also influence habitat quality. Our findings that fisher distribution was best predicted by vegetation + climate models—whereas there was no significant difference between vegetation + climate, climate-only, or vegetation-only models for marten—may reflect differences in vegetation disturbance patterns in the elevation zones occupied by the two species. Forests in the midelevation zone occupied by fishers have experienced much greater human-induced changes in vegetation structure and composition since Euro-American colonization in the Sierra Nevada compared to the higher-elevation forests occupied by martens. This is due in part to more intensive logging, fire suppression, and other management actions in mid-elevation compared to higher-elevation forests—as well as the protection of

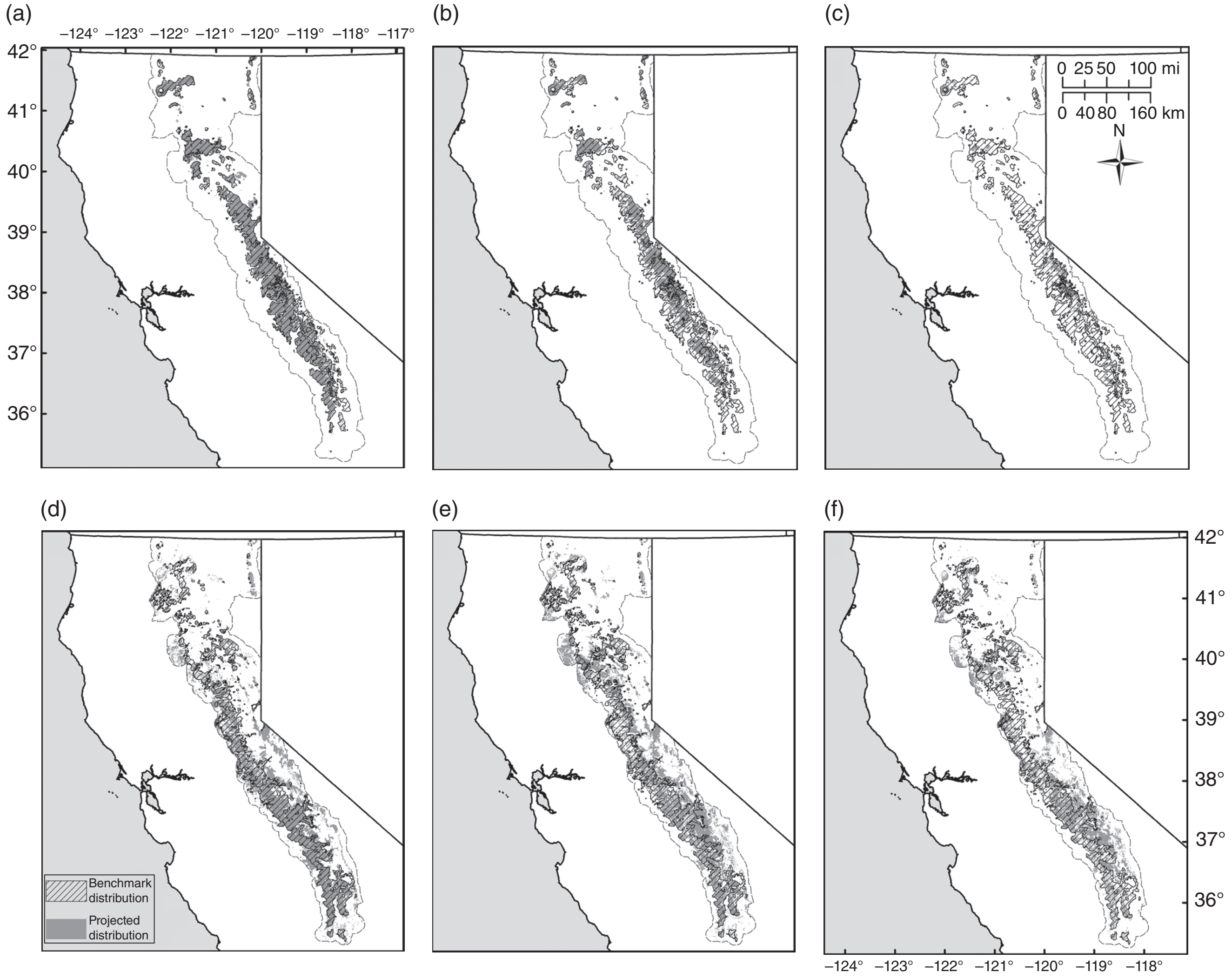

Figure 9.5 Predicted marten [top row, maps (a)–(c)] and fisher [bottom row, maps (d)–(f)] distributions under climate change projections from the MIROC 3.2 medres with the A2 emission scenario at 800 × 800-m resolution. Maps (a) and (d) show contemporary distributions (1986–2005); maps (b) and (e) show midcentury (2046–2065); maps (c) and (f) show late century (2076–2095). Hatched overlay shows the benchmark distribution based on the best current distribution models with 10-km^2 moving-window averaging. For color details, please see color plate section.

Table 9.6 Net change and stable range for marten and fisher distribution projections at 800 × 800-m resolution for three scenarios and two future time periods.

		CSIROMk3 A2		Hadley CM3 A2		MIROC 3.2 medres A2	
Species		2046–2065	2076–2095	2046–2065	2076–2095	2046–2065	2076–2095
Marten	Net change	−0.20	−0.40	−1.00	−0.85	−0.46	−0.84
	Stable range	0.60	0.38	0.00	0.11	0.52	0.14
Fisher	Net change	0.14	0.38	−0.11	0.12	−0.01	−0.33
	Stable range	0.62	0.60	0.50	0.52	0.59	0.40

much more land in national parks and wilderness areas at higher elevations [*Beesley*, 1996]. The stronger influence of management actions on forest condition in the range of fishers may have partially decoupled the correlation between vegetation and climate within the fisher's elevation band: Whereas climate alone is a good general predictor of where fishers occur, adding vegetation characteristics improves the predictive power of distribution models.

Other recent studies have also shown the importance of considering both vegetation variables and climate variables in species distribution models, especially in human-altered ecosystems. *Barbet-Massin et al.* [2012] found that model accuracy is better, and explanatory power higher, for models combining climate and vegetation variables compared to climate-only or vegetation-only models for numerous taxa in Europe at 50-km resolution. *Sohl* [2014] also found that landcover + climate models provide better fit than do either landcover or climate-only models for 50 bird species in the US. Using climate data alone resulted in broad, generalized distributions, and adding landcover variables decreased predicted suitable area for most species, in large part due to human alterations of landcover.

Once the effects of climate and vegetation were included in a marten or fisher distribution model, adding presence or absence of the other species did not contribute significantly to model predictive power. These results suggest that martens and fishers primarily select habitats according to appropriate climate and vegetation conditions, rather than the presence or absence of the other species. Presence of fishers may affect some individual martens in their narrow contact zone, but does not appear to be a current driving factor behind the distribution of marten populations. Evidence from telemetry and survey data suggest that fishers slightly contract their habitat use downslope during the snowy season (perhaps to avoid deeper or softer snows at higher elevations) and expand upslope again during snow-free seasons [*Spencer et al.*, 2015], whereas martens expand their ranges downslope during the snowy season, and contract upslope during warmer, snow-free seasons (perhaps to avoid high temperatures) [*Zielinski et al.*, 2015]. Although these expansions and contractions tend to minimize species range overlap year-round, they appear to be influenced more by climate than by presence or absence of the other species, because martens exhibit this pattern even in regions lacking fishers [*Zielinski et al.*, 2015].

9.4.2. Current Distributions Using MC1-Based Variables

Not surprisingly, the finest available downscaled GCM resolution (800 m) performed the best at predicting current distributions of both species. As also found by *Franklin et al*. [2012] for numerous plant species, we saw large overpredictions of marten distributions at coarser resolutions (Figure 9.2a–c). However, this pattern was not consistent for fisher distributions (Figure 9.2d–f). This may be due to the relatively poor performance of MC1-derived vegetation variables in reproducing benchmark model projections, coupled with the greater permutation importance of vegetation variables in fisher models. Because different MC1-derived vegetation variables entered the best models at each resolution, this variability increases uncertainties in fisher model projections both within and between the three resolutions.

Similar to the marten benchmark models, climate variables proved to be very good predictors of marten distribution in the MC1-based models (accounting for 76.4% of the permutation importance for the 800-m model); and adding vegetation variables did not contribute much to model performance (only 23.6% of permutation importance). However, for fishers, the apparent decoupling of vegetation-climate correlations due to greater human influences on their habitat may make contributions from vegetation variables more important in modeling performance. Hence, if MC1-derived vegetation variables are not strong reflections of on-ground habitat conditions compared to our best available vegetation variables from other sources, this could adversely affect model performance for fishers, and greatly add to uncertainties in future projections of fisher distribution.

9.4.3. Future Projections

There are large uncertainties about future climate and vegetation conditions in the Sierra Nevada, due to differences among the different GCM and emission scenarios used for projections [*Lenihan et al.*, 2008; *Hayhoe et al.*, 2004]. Climate models agree over the general warming trend in the western US, but projections of precipitation are much less certain, increasing uncertainties in projections of future drought stress, fuels conditions, and fire hazards [*Westerling and Bryant*, 2008]. Projections of snowpack depth and duration are also highly uncertain [*Mote*, 2006; *Kapnick and Hall*, 2012). Climate projections from the fifth assessment report indicate declines in spring snow cover and increases in summer temperatures [e.g., *Peacock*, 2011]. Ensemble means indicate that the CMIP5 model runs over the western US do not show any lessening of the trends already projected for the fourth assessment report [*IPCC*, 2007, 2013). Increased climate variability may allow for some very high snow years as well as extremely low snow years.

How marten and fisher populations may respond to these potential changes is also uncertain. Decreasing snow cover may benefit fishers, which are not as well adapted to deep, soft, or persistent snow, due to higher foot-loading [*Krohn et al.*, 1997, 2004]; but increasing temperatures and temperature variability are likely detrimental to both species, which seek out habitats with cool, mesic microclimates and low-temperature amplitudes. How increased interannual variability in precipitation and snowpack may affect the species is unknown, but they may increase the amplitude of population fluctuations and extinction risks in both species. *Lawler et al.* [2012] created climate-envelope models to detect shifts for martens and fishers across their entire North American ranges in response to projected changes in temperature and precipitation using coarse resolution (50-km) climate data without considering effects of topography or vegetation. Their results showed contractions along southern portions of the species' ranges and that both species will lose most of their climatically suitable range in the contiguous United States by the end of this century.

Future decoupling of climate envelopes from vegetation conditions, due to vegetation response lags, may spell even greater trouble for species such as martens and fishers whose niches are influenced by both. *Barbet-Massin et al.* [2012] and Sohl [2014] found that climate-only models predict larger shifts in future range size than do landcover-only models, and our projections for martens show some evidence of future decoupling having adverse effects, at least for martens. In our models, all three GCMs (CSIRO Mk3, Hadley CM3, and MIROC 3.2 medres) using the A2 emissions scenario paint a rather dire future picture for martens in the Sierra Nevada (Figures 9.3–9.5), with major contractions and fragmentation in predicted distribution. In the Hadley CM3 projections, a major contraction in marten distribution by the mid-21st century (Figure 9.4b) is followed by a slight expansion again by the end of the century (Figure 9.4c). The midcentury contraction may reflect a bottleneck for marten populations due to decoupling of the species' preferred climatic vs. vegetation conditions as the climate shifts more rapidly than vegetation can respond.

The apparent historical decoupling of climate-vegetation associations for fishers, due to human influences on vegetation conditions, has already increased uncertainties in both current and future distribution projections. Further decoupling due to climate change is likely to have adverse effects on both martens and fishers. However, these correlation analyses cannot attribute cause-effect relations, and it remains unknown whether martens and fishers will abandon current vegetation community associations to stay within preferred climate envelopes (as long as forest structural conditions are appropriate). Also, complex topography can cause microclimate conditions that are not represented by interpolated climate from a limited number of meteorological stations, allowing some decoupling from regional climate [*Daly et al.*, 2010]. Complex terrain in the Sierra Nevada may cause inversions and cold-air ponding, for example, which may result in refugia with appropriate climate and vegetation conditions that cannot be predicted with the current models.

9.4.4. Conclusions

Based on the results of these analyses and our general knowledge of marten and fisher ecology, we suspect that the distribution of martens is likely to significantly decrease and become more fragmented in the future. Martens may persist in areas that retain deep, persistent snow and some dense forest patches with large trees, perhaps in high-elevation canyons and valleys. The future of fishers is even more uncertain, with model projections based on the different GCM emission scenarios showing either distribution expansions or contractions. Conservation actions for these species should consider how management may be able to help sustain appropriate vegetation conditions within the climate envelopes required by each species while sustaining or increasing overall ecosystem resilience in the face of climate change. It won't be easy, and it will require management to adapt as conditions change.

ACKNOWLEDGMENTS

The authors want to acknowledge the Yale Framework for Biodiversity Conservation and Climate Adaptation for funding the analyses presented here, which built on previous work funded by the Resources Legacy Foundation and an anonymous donor. William Zielinski, Tom Kirk, and Ric Schlexer helped assemble marten and fisher locality data and provided insights into marten and fisher ecology. This chapter was greatly improved by comments from two anonymous reviewers.

REFERENCES

Bachelet D., R. P. Neilson, J. M. Lenihan, and R. J. Drapek (2001), Climate change effects on vegetation distribution and carbon budget in the U.S., *Ecosystems*, *4*, 164–185.

Barbet-Massin, M., W. Thuiller, and F. Jiguet (2012), The fate of European breeding birds under climate, land-use and dispersal scenarios, *Global Change Biol.*, *18*, 881–890.

Beesley, D. (1996), Reconstructing the landscape: An environmental history, 1820–1960, in *Sierra Nevada Ecosystem Project Final Report to Congress,* Vol. II, *Assessments and Scientific Basis for Management Options*, Centers for Water and Wildlife Resources, University of California, Davis, pp. 3–24.

CNDDB (California Department of Fish and Game, Biogeographic Data Branch) (2011), *California Natural Diversity Database*, Sacramento, CA (data downloaded Nov. 2011).

Conklin, D. C. (2009), *Simulating Vegetation Shifts and Carbon Cycling in Yosemite National Park*, PhD thesis, Oregon State University, Corvallis.

Daly, C., D. R. Conklin, and M. H. Unsworth (2010), Local atmospheric decoupling in complex topography alters climate change impacts, *Int. J. Climatol.*, *30*, 1857–1864.

Davis, F., C. Seo, and W. J. Zielinski (2007), Regional variation in home-range scale habitat models for fisher (*Martes pennanti*) in California, *Ecol. Applications*, *178*, 2195–2213.

Elith J., S. J. Phillips, T. Hastie, M. Dudik, Y. E. Chee, and C. J. Yates (2011), A statistical explanation of MaxEnt for ecologists, *Diversity Distributions*, *17*, 43–57.

Fielding, A. H., and J. F. Bell (1997), A review of methods for the assessment of prediction errors in conservation presence/absence models, *Environ. Conservation*, *24*, 38−49.

Franklin, J. (2003), Clustering versus regression trees for determining ecological land units in the southern California mountains and foothills, *Forest Sci.*, *49*, 354−368.

Franklin, J., F. W. Davis, M. Ikegami, A. D. Syphard, L. E. Flint, Al L. Flint, and L. Hannah (2012), Modeling plant species distributions under future climates: How fine scale do climate projections need to be? *Global Change Biol.*, *19*, 473–483, doi:10.1111/gcb.12051.

Gordon, H. B., L. D. Rotstayn, J. L. McGregor, M. R. Dix, E. A. Kowalczyk, S. P. O'Farrell, L. J. Waterman, A. C. Hirst, S. G. Wilson, M. A. Collier, I. G. Watterson, and T. I. Elliott (2002), *The CSIRO Mk3 Climate System Model,* CSIRO Atmospheric Research Technical Paper 60.

Gordon, C., C. Cooper, C. A. Senior, H. Banks, J. M. Gregory, T. C. Johns, J. F. B. Mitchell, and R. A. Wood (2000), The simulation of SST, sea ice extents and ocean heat transports in a version of the Hadley Centre coupled model without flux adjustments, *Climate Dynamics*, *16*, 147–168.

Gustafson, E. J., S. M. Lietz, and J. L. Wright (2003), Predicting the spatial distribution of aspen growth potential in the upper Great Lakes region, *Forest Sci.*, *49*(4), 499−508.

Hasumi, H., and S. Emori (eds.) (2004), *K-1 Coupled GCM (MIROC) Description*, K-1 Technical Report 1, Center for Climate Systems Research, Tokyo (available online at http://www.ccsr.u-tokyo.ac.jp/kyosei/hasumi/MIROC/tech-repo.pdf).

Hayhoe, K., D. Cayan, C. B. Field, P. C. Frumhoff , E. P. Maurer, N. L. Miller, S. C. Moser, S. H. Schneider, K. Nicholas Cahill, E. E. Cleland, L. Dale, R. Drapek, R. M. Hanemann, L. S. Kalkstein, J. Lenihan, C. K. Lunch, R. P. Neilson, S. C. Sheridan, and J. H. Verville (2004), Emissions pathways, climate change, and impacts on California, *Proc. Natl. Acad. Sci.*, *101*, 12422−12427.

IPCC (2007), Summary for policymakers, in S. D. Solomon, D. Qin, M. Manning, Z. Chen, K. B. Averyt, M. Marquis, M. Tignor, and H. L. Miller (eds.), *Climate Change 2007: The Physical Science Basis. Contribution of Working Group I to the Fourth Assessment Report of the Intergovernmental Panel on Climate Change*, Cambridge University Press, Cambridge, UK and New York.

IPCC (2013), in T. F. Stocker, D. Qin, G.-K. Plattner, M. Tignor, S. K. Allen, J. Boschung, A. Nauels, Y. Xia, V. Bex, and P. M. Midgley (eds.), *Climate Change 2013: The Physical Science Basis. Contribution of Working Group I to the Fifth Assessment Report of the Intergovernmental Panel on Climate Change*, Cambridge University Press, Cambridge, UK and New York.

Johns, T. C., J. M. Gregory, W. J. Ingram, C. E. Johnson, A. Jones, J. A. Lowe, J. F. B. Mitchell, D. L. Roberts, D. M. H. Sexton, D. S. Stevenson, S. F. B. Tett, and M. J. Woodage (2003), Anthropogenic climate change for 1860 to 2100 simulated with the HadCM3 model under updated emissions scenarios, *Climate Dynamics*, *20*, 583−612.

Kapnick, S., and A. Hall (2012), Causes of recent changes in western North American snowpack, *Climate Dynamics*, *38*, 1885−1899.

Kirk, T. A., and W. J. Zielinski (2009), Developing and testing a landscape habitat suitability model for the American marten (*Martes americana*) in the Cascades mountains of California, *Landscape Ecol.*, *24*, 759−773

Krohn, W. B., C. Hoving, D. Harrison, D. Phillips, and H. Frost (2004), *Martes* foot-loading and snowfall patterns in eastern North America: Implications to broad-scale distributions and interactions of mesocarnivores, in D. J. Harrison et al. (eds.), *Martens and Fishers (Martes) in Human-altered Environments: An International Perspective*, Springer, New York, USA, pp. 115–131.

Krohn, W. B., W. J. Zielinski, and R. B. Boone (1997), Relations among fishers, snow and martens in California: Results from small-scale spatial comparisons, in G. Proulx et al. (eds.), *Martes: Taxonomy, Ecology, Techniques, and Management*, Provincial Museum of Alberta, Edmonton, Alberta, Canada, pp. 211−232.

Lawler, J. J., H. D. Safford, and E. H. Girvetz (2012), Martens and fishers in a changing climate, in K. B. Aubry (ed.), *Biology and Conservation of Martens, Sables, and Fishers: A New Synthesis*, Cornell University Press.

Legendre, P., and L. Legendre (1998), Numerical *Ecology*, 2nd English ed., Elsevier Science BV, Amsterdam.

Lenihan, J. M., D. Bachelet, R.J. Drapek, and R. P. Neilson (2008), The response of vegetation distribution, ecosystem productivity, and fire in California to future climate scenarios simulated by the MC1 dynamic vegetation model, *Climatic Change*, *87*(Suppl. 1), S215−S230.

Liu, C., M. White, and G. Newell (2013), Selecting thresholds for the prediction of species occurrence with presence-only data, *J. Biogeogr.*, *40*(4), 778−789.

Matthews, S. N., L. R. Iverson, A. M. Prasad, and M. P. Peters (2011), Changes in potential habitat of 147 North American breeding bird species in response to redistribution of trees and climate following predicted climate change, *Ecography*, *34*, 933–945.

Meehl, G. A., W. M. Washington, T. M. L. Wigley, J. M. Arblaster, and A. Dai (2003), Solar and greenhouse gas forcing and climate response in the twentieth century, *J. Climate*, *16*, 426–444.

Meehl, G. A., C. Covey, T. Delworth, M. Latif, B. McAvaney, J. F. B. Mitchell, R. J. Stouffer, and K. E. Taylor (2007), The WCRP CMIP3 multi-model dataset: A new era in climate change research, *Bull. Am. Meteorol. Soc.*, *88*, 1383−1394.

Mote, P. (2006), Climate driven variability and trends in mountain snowpack in western North America, *Am. Meteorol. Soc.*, *19*, 6209−6220.

Nakićenović, N., J. Alcamo, G. Davis, B. de Vries, J. Fenhann, S. Gaffin, K. Gregory, A. Grübler, T. Y. Jung, T. Kram, E. Lebre La Rovere, L. Michaelis, S. Mori, T. Morita, W. Pepper, H. Pitcher, L. Price, K. Riahi, A. Roehrl, H.-H. Rogner, A. Sankovski, M. Schlesinger, P. Shukla, S. Smith, R. Swart, S. van Rooijen, N. Victor, and Z. Dadi (2000), *Special Report on Emissions Scenarios: A Special Report of Working Group III of the Intergovernmental Panel on Climate Change*, Cambridge University Press, Cambridge, UK.

Peacock, S. (2011), Projected 21st century climate change for wolverine habitats within the. contiguous United States, *Environ. Research Lett.*, *6*, 1–9, doi:10.1088/1748-9326/6/1/014007.

Phillips, S. (2006), *A Brief Tutorial on Maxent*, AT&T Research (available at http://www.cs.princeton.edu/~schapire/maxent/tutorial/tutorial.doc).

Phillips, S. J., R. P. Anderson, and R. E. Shapire (2006), Maximum entropy modeling of species geographic distributions, *Ecol. Model.*, *190*, 231–259.

Pope, V. D., M. L. Gallani, P. R. Rowntree, and R. A. Stratton (2000), The impact of new physical parameterisations in the Hadley Centre climate model–HadAM3, *Climate Dynamics*, *16*, 123–146.

Purcell, K. L., C. M. Thompson, and W. J. Zielinski (2012), Fishers and American martens, in M. North (ed.), *Managing Sierra Nevada Forests*, General Technical Report PSW-GTR-237, USDA Forest Service, Pacific Southwest Research Station, Albany, CA, pp. 47−60.

Sappington, J. M., K. M. Longshore, and D. B. Thomson (2007), Quantifying landscape ruggedness for animal habitat analysis: A case study using bighorn sheep in the Mojave Desert, *J. Wildlife Management*, *71*(5),1419−1426.

Sohl, T. L. (2014), The relative impacts of climate and land-use change on conterminous United States bird species from 2001 to 2075, *PLoS ONE*, *9*(11), 1−18.

Spencer, W. D. (1987), Seasonal rest-site preferences of pine martens in the northern Sierra Nevada, *J. Wildlife Management*, *51*, 616−621.

Spencer, W. D., S. C. Sawyer, H. L. Romsos, W .J. Zielinski, R. A. Sweitzer, C. M. Thompson, K. L. Purcell, D. L. Clifford, L. Cline, H. D. Safford, S. A. Britting, and J. M. Tucker (2015), *Southern Sierra Nevada Fisher Conservation Assessment*, unpublished report produced by Conservation Biology Institute, Jan. 2015.

Washington, W. M., J. W. Weatherly, G. A. Meehl, A. J. Semtner, T. W. Bettge, A. P. Craig, W. G. Stran, J. Arblaster, V. B. Wayland, R. James , and Y. Zhang (2000), Parallel climate model (PCM) control and transient simulations, *Climate Dynamics*, *16*, 755–774.

Westerling, A.L., H. G. Hidalgo, D. R. Cayan, and T. W. Swetnam (2006), Warming and earlier spring increase western U.S. forest wildfire activity, *Science*, *313*(5789), 940−943.

Westerling, A. L., and B. P. Bryant (2008), Climate change and wildfire in California, *Climatic Change*, *87*(Suppl 1), s231−s249.

Zielinski, W. J., W. D. Spencer, and R. H. Barrett (1983), Relationship between food habits and activity patterns of pine martens, *J. Mammal.*, 64, 387–396.

Zielinski, W. J., and N. P. Duncan (2004), Diets of sympatric populations of American martens (*Martes americana*) and fishers (*Martes pennanti*) in California, *J. Mammal.*, *85*(3), 470−477.

Zielinski, W. J., R. L. Truex, F. V. Schlexer, L. A. Campbell, and C. Carroll (2005), Historical and contemporary distributions of carnivores in forests of the Sierra Nevada, California, *J. Biogeogr.*, *32*, 1385−1407.

Zielinski, W. J., K. M. Moriarty, K. M. Slauson, J. Baldwin, T. A. Kirk, H. L. Rustigian-Romsos, and W. D. Spencer (2015), Effects of season on Pacific marten occupancy and implications for habitat modeling, *Wildlife Biol*, *21*, 56–67.